we employed the PolyWare technique instead. As reported by Stilling et al., mean PE wear measured with PolyWare tends to be greater than that measured using the RSA method [31]. Consequently, the present study possibly overestimated the amount of penetration.

Fourth, among all patients, 38 (50%) had negative wear between 1 and 3 years. Such results are common in short-term studies of HXLPE liners [19,23,24]. Engh et al. reported a negative wear rate in 32% of the patients in their study [19]. As Lachiewicz et al. pointed out, these paradoxical observations should be attributed to the detection limits of the measurement technique [23].

Fifth, we used 26-mm-diameter Co–Cr–Mo alloy heads on the femoral side. However, in the clinical setting, various femoral heads of larger sizes and materials are available. Although we confirmed that improvements due to PMPC grafting surpassed those due to changes in the femoral head sizes or materials in the hip joint simulator studies [32], the outcome of THR using other femoral heads should be evaluated to determine the clinical utility of PMPC-grafted HXLPE liners. A multicenter study (UMIN000008730) is currently underway for the evaluation of other femoral heads, including zirconia-toughened alumina ceramic femoral heads and femoral heads with a larger diameter [33].

In conclusion, this study demonstrated that use of a PMPC-grafted HXLPE liner in THR appears to provide good clinical and radiographic results at 3 years after the index surgery. Further follow-up is needed to determine whether PMPC-grafted HXLPE liners improve long-term clinical outcomes.

Acknowledgments

The authors would like to thank the late Dr. Shuhei Morimoto for his invaluable contribution and participation in the present study since 2006.

Conflict of interest

One or more of the authors or institutions received outside funding or grants from KYOCERA Medical Corporation. One of the authors (K.M.) is employed by KYOCERA Medical Corporation.

References

1. Willert HG, Bertram H, Buchhorn GH. Osteolysis in alloarthroplasty of the hip. The role of ultra-high molecular weight polyethylene wear particles. Clin Orthop Relat Res. 1990;258:95–107.
2. Kirk TB, Wilson AS, Stachowiak GW. The morphology and composition of the superficial zone of mammalian articular cartilage. J Orthop Rheumatol. 1993;6:21–8.
3. Hills BA. Boundary lubrication in vivo. Proc Inst Mech Eng [H]. 2000;214:83–94.
4. Moro T, Takatori Y, Ishihara K, Konno T, Takigawa Y, Matsushita T, et al. Surface grafting of artificial joints with a biocompatible polymer for preventing periprosthetic osteolysis. Nat Mater. 2004;3(11): 829–36.
5. Moro T, Takatori Y, Ishihara K, Nakamura K, Kawaguchi H. Grafting of biocompatible polymer for longevity of artificial hip joints. Clin Orthop Relat Res. 2006;453:58–63.
6. Moro T, Kyomoto M, Ishihara K, Saiga K, Hashimoto M, Tanaka S, et al. Grafting of poly (2-methacryloyloxyethyl phosphorylcholine) on polyethylene liner in artificial hip joints reduces production of wear particles. J Mechan Behav Biomed Mater. 2014;31:100–6.
7. Moro T, Takatori Y, Kyomoto M, Ishihara K, Hashimoto M, Ito H, et al. Long-term hip simulator testing of the artificial hip joint bearing surface grafted with biocompatible phospholipid polymer. J Orthop Res. 2014;32(3):369–76.
8. Kyomoto M, Moro T, Saiga K, Hashimoto M, Ito H, Kawaguchi H, et al. Biomimetic hydration lubrication with various polyelectrolyte layers on cross-linked polyethylene orthopedic bearing materials. Biomaterials. 2012;33(18):4451–9.
9. Myers GJ, Johnstone DR, Swyer WJ, McTeer S, Maxwell SL, Squires C, et al. Evaluation of Mimesys phosphorylcholine (PC)-coated oxygenators during cardiopulmonary bypass in adults. J Extra Corpor Technol. 2003;35(1):6–12.
10. Kuiper KK, Nordrehaug JE. Early mobilization after protamine reversal of heparin following implantation of phosphorylcholine-coated stents in totally occluded coronary arteries. Am J Cardiol. 2000;85(6):698–702.
11. Selan L, Palma S, Scoarughi GL, Papa R, Veeh R, Di Clemente D, Artini M. Phosphorylcholine impairs susceptibility to biofilm formation of hydrogel contact lenses. Am J Ophthalmol. 2009; 147(1):134–9.
12. Snyder TA, Tsukui H, Kihara S, Akimoto T, Litwak KN, Kameneva MV, et al. Preclinical biocompatibility assessment of the EVAHEART ventricular assist device: Coating comparison and platelet activation. J Biomed Mater Res A. 2007;81(1):85–92.
13. Takatori Y, Moro T, Kamogawa M, Oda H, Morimoto S, Umeyama T, et al. Poly(2-methacryloyloxyethyl phosphorylcholine)-grafted highly cross-linked polyethylene liner in primary total hip replacement: one-year results of a prospective cohort study. J Artif Organs. 2013;16(2):170–5.
14. Charnley J. The long-term results of low-friction arthroplasty of the hip performed as a primary intervention. J Bone Joint Surg Br. 1972;54(1):61–76.
15. Imura S. Evaluation chart of hip join functions. J Jpn Orthop Assoc. 1995;69:860–7.
16. Fujisawa M, Naito M, Asayama I. A comparative study of hip joint functional scoring systems between Japanese Orthopaedic Association hip score and Harris hip score. Seikeigeka. 2001;52: 628–33 (in Japanese).
17. Nagai I, Takatori Y, Kuruta Y, Moro T, Karita T, Mabuchi A, Nakamura K. Nonself-centering Bateman bipolar endoprosthesis for nontraumatic osteonecrosis of the femoral head: a 12- to 18-year follow-up study. J Orthop Sci. 2002;7(1):74–8.
18. Sutherland CJ, Wilde AH, Borden LS, Marks KE. A ten-year follow-up of one hundred consecutive Müller curved-stem total hip-replacement arthroplasties. J Bone Joint Surg Am. 1982;64(7):970–82.
19. Engh CA Jr, Stepniewski AS, Ginn SD, Beykirch SE, Sychterz-Terefenko CJ, Hopper RH Jr, Engh CA. A randomized prospective evaluation of outcomes after total hip arthroplasty using cross-linked marathon and non-cross-linked Enduron polyethylene liners. J Arthroplasty. 2006;21(Suppl 2):17–25.
20. Hui AJ, McCalden RW, Martell JM, MacDonald SJ, Bourne RB, Rorabeck CH. Validation of two and three-dimensional radiographic techniques for measuring polyethylene wear after total hip arthroplasty. J Bone Joint Surg Am. 2003;85(3):505–11.
21. Glyn-Jones S, McLardy-Smith P, Gill HS, Murray DW. The creep and wear of highly cross-linked polyethylene: a three-year randomised, controlled trial using radiostereometric analysis. J Bone Joint Surg Br. 2008;90(5):556–61.
22. Calvert GT, Devane PA, Fielden J, Adams K, Horne JG. A double-blind, prospective, randomized controlled trial comparing highly cross-linked and conventional polyethylene in primary total hip arthroplasty. J Arthroplasty. 2009;24(4):505–10.
23. Lachiewicz PF, Heckman DS, Soileau ES, Mangla J, Martell JM. Femoral head size and wear of highly cross-linked polyethylene at 5 to 8 years. Clin Orthop Relat Res. 2009;467(12):3290–6.
24. Whittaker JP, Charron KD, McCalden RW, Macdonald SJ, Bourne RB. Comparison of steady state femoral head penetration rates between two highly cross-linked polyethylenes in total hip arthroplasty. J Arthroplasty. 2010;25(5):680–6.
25. Capello WN, D'Antonio JA, Ramakrishnan R, Naughton M. Continued improved wear with an annealed highly cross-linked polyethylene. Clin Orthop Relat Res. 2011;469(3):825–30.
26. Udomkiat P, Wan Z, Dorr LD. Comparison of preoperative radiographs and intraoperative findings of fixation of hemispheric porous-coated sockets. J Bone Joint Surg Am. 2001;83A(12):1865–70.
27. Kyomoto M, Moro T, Konno T, Takadama H, Kawaguchi H, Takatori Y, et al. Effects of photo-induced graft polymerization of 2-methacryloyloxyethyl phosphorylcholine on physical properties of cross-linked polyethylene in artificial hip joints. J Mater Sci Mater Med. 2007;18(9):1809–15.
28. Collier JP, Currier BH, Kennedy FE, Currier JH, Timmins GS, Jackson SK, Brewer RL. Comparison of cross-linked polyethylene materials for orthopaedic applications. Clin Orthop Relat Res. 2003;414:289–304.
29. Medel FJ, Peña P, Cegoñino J, Gómez-Barrena E, Puértolas JA. Comparative fatigue behavior and toughness of remelted and annealed

highly crosslinked polyethylenes. J Biomed Mater Res B Appl Biomater. 2007;83(2):380–90.
30. Kärrholm J, Herberts P, Hultmark P, Malchau H, Nivbrant B, Thanner J. Radiostereometry of hip prostheses. Review of methodology and clinical results. Clin Orthop Relat Res. 1997;344:94–110.
31. Stilling M, Larsen K, Andersen NT, Søballe K, Kold S, Rahbek O. The final follow-up plain radiograph is sufficient for clinical evaluation of polyethylene wear in total hip arthroplasty. A study of validity and reliability. Acta Orthop. 2010;81(5):570–8.
32. Moro T, Kawaguchi H, Ishihara K, Kyomoto M, Karita T, Ito H, et al. Wear resistance of artificial hip joints with poly(2-methacryloyloxyethyl phosphorylcholine) grafted polyethylene: Comparisons with the effect of polyethylene cross-linking and ceramic femoral heads. Biomaterials. 2009;30(16):2995–3001.
33. Kurtz SM, Kocagöz S, Arnholt C, Huet R, Ueno M, Walter WL. Advances in zirconia toughened alumina biomaterials for total joint replacement. J Mech Behav Biomed Mater. 2014; 31:107–16.

Tribology Online
Japanese Society of Tribologists

Tribology Online, 10, 1 (2015) 1-10.
ISSN 1881-2198
DOI 10.2474/trol.10.1

Article

Investigation on Oxidation of Shelf-Aged Crosslinked Ultra-High Molecular Weight Polyethylene (UHMWPE) and Its Effects on Wear Characteristics

Lei Zhang[1)*], Yoshinori Sawae[2,3)], Tetsuo Yamaguchi[2)], Teruo Murakami[3)], Hong Yang[1)]
[1)]Graduate School of Engineering, Kyushu University
744 Motooka, Nishi-ku, Fukuoka 819-0395, Japan
[2)]Faculty of Engineering, Kyushu University
744 Motooka, Nishi-ku, Fukuoka 819-0395, Japan
[3)]Research Center for Advanced Biomechanics, Kyushu University
744 Motooka, Nishi-ku, Fukuoka 819-0395, Japan
[*]Corresponding author: zhanglei8609@hotmail.com

(Manuscript received 9 May 2014; accepted 15 November 2014; published 15 January 2015)

Oxidation degradation of gamma-irradiated UHMWPE (Ultra-high Molecular Weight Polyethylene) is a well-known problem related to the failure of total joint replacement. The purpose of this study is to investigate the effects of oxidation on the mechanical and wear properties and to identify the main causes of the change of wear mechanisms of crosslinked UHMWPE (50 kGy and 100 kGy) after long-term shelf-ageing. The techniques used were FTIR mapping and micro-indentation test, which were performed on the same cross-section of UHMWPE specimen. Three distinct regions (the surface region, the more oxidized subsurface region, and the less oxidized center region) were prepared to carry out the differential scanning calorimetry (DSC) and multi-directional wear tests. The worn surfaces were checked by optical microscopy and scanning electron microscopy to reveal the wear mechanisms. The experimental results showed that the micro-hardness, elastic modulus and crystallinity increased with the increase of the oxidation index. The wear resistance deteriorated when the oxidation index increased. The slope of specific wear rate against oxidation index of the 100 kGy sample is higher than that of the 50 kGy sample. Our results may indicate that, when the oxidation index is lower than the critical threshold, the wear mechanism is mainly dependent on crosslinking density; when the oxidation index is higher than the critical threshold, the oxidation behavior plays an important role in the change of wear mechanisms.

Keywords: UHMWPE, wear, oxidation, crosslinking, gamma-irradiation, shelf-ageing

1. Introduction

It is now acknowledged that the wear of UHMWPE (Ultra-high Molecular Weight Polyethylene) is a main factor restricting the service life of total joint prosthesis. Thus, numerous studies dealing with microstructure and mechanical properties of UHMWPE to eliminate wear of this polymer were developed [1-4]. Among them, the most popular and successful technique to improve the wear-resistance is to crosslink the UHMWPE by gamma radiation [5-7].

However, free radicals, which are susceptible to oxidation degradation that alters the physical, chemical, and mechanical properties of UHMWPE, are generated along the backbone of the UHMWPE molecule through breaking C-C and C-H bonds within the amorphous and crystalline phases during gamma irradiation [8]. The free radicals are supposed to recombine with each other to form the crosslinks, but not all of the free radicals are mobile enough to recombine with each other. In fact, the free radicals formed in crystalline phases of the UHMWPE are thought to be trapped and react with oxygen to cause oxidation in the long term [8,9]. Thermal treatment on post-irradiated UHMWPE is generally applied to eliminate the residual free radicals and alleviate the oxidation degradation [5,10]. Remelting above the melting point of UHMWPE is capable to eliminate the residual free radicals to undetectable level and is effective in preventing the UHMWPE component from oxidizing, but diminishes fatigue crack propagation resistance. Annealing below the melting point can also reduce the amount of free radicals, delay the oxidation, and results in better wear and fatigue resistance compared to the remelting method. However, some free radicals remain and the long-term oxidative degradation is hardly prevented.

In addition, the generated free radical concentration has been proved to be proportional to the radiation dose

[11,12] and crosslinked UHMWPEs with different dose levels probably differ from each other in the oxidation behavior. O'Neill et al. [13] found that the maximum oxidation occurred close to the surface and its value and position were dose-dependent, however the related mechanical and wear properties were not referred in his paper. Furthermore, the UHMWPE components are usually stored for a period of time due to business needs. Currier et al. [14] and Kyomoto et al. [15] reported that the shelf time before implantation appears to be a significant factor in the success or failure of UHMWPE bearings that are gamma sterilized in air. Fisher et al. [16] and Toohey et al. [17] also reported that crosslinked UHMWPE had a higher wear rate after ageing.

The oxygen concentration, which related to the oxidation, is influenced by the storage condition and *in vivo* condition. During 1990s, most of the UHMWPE components were packaged and stored in an air-permeable condition, which is roughly 8 times the oxygen content *in vivo* [18]. Due to the higher oxygen content compared with *in vivo* condition, the oxidation occurred during the shelf-storage is assumed to be the key factor in the wear resistance of the UHMWPE components [15]. Although the UHMWPE components are packaged in reduced oxygen environment after 1998, all the polymer materials commonly used for packaging are proved to be permeable to oxygen [19]. Thus, a variable amount of oxygen could be available to cause the oxidation. Besides, there are a lot of crosslinked UHMWPE components shelf-stored without barrier packaging in use. Therefore, it is meaningful to know the effect of oxidation on the mechanical and wear properties of shelf-aged crosslinked UHMWPE materials.

Despite valuable studies about the wear behavior of gamma-irradiated UHMWPE derived from earlier researchers, in-depth investigation of the relationship between the oxidation, mechanical properties and wear behavior of shelf-aged crosslinked UHMWPE is scarce. In this study, gamma-irradiated (dose level: 50 kGy, 100 kGy) and annealed UHMWPEs, which were shelf-aged for 7 years, were chosen as the research objects. The main objectives were to evaluate the effects of oxidation on mechanical and wear properties of crosslinked UHMWPE, and to identify the main causes of the change of wear mechanisms.

2. Experimental procedure

2.1. Material selection and preparation

Compression-moulded GUR 1050 UHMWPE rods with a molecular weight of 5.5-6 million-g/mol and a density of 0.93 g/cm^3 were chosen as the testing material in this paper. The UHMWPE rods were irradiated in air at room temperature with gamma rays from cobalt 60 to the total dose of 50 kGy and 100 kGy which are commonly used on the UHMWPE crosslinking and the dose rate is 10 kGy/h. After irradiation, the rods were annealed by heating at 110°C for 8 hours inside a vacuum oven, and then slowly cooled down in the oven to ambient temperature over a period of 24 hours. Any surface oxidation products that occurred during the in-air irradiation were removed prior to machining into the final cylinder shape with a diameter of 6 mm and a length of 15 mm. Finally, all specimens without sterilization were shelf-aged at ambient temperature in an air-containing double PE package for 7 years. The non-crosslinked UHMWPE cylinder with non-shelf-ageing was used as control sample.

2.2. Characterization techniques

The shelf-aged specimens were initially cut in half and microtomed along the radial direction by using the Leica RM 2125 RTS manual microtome at ambient temperature to obtain flat and smooth cross-sections for the following tests. A Fourier transform infrared (FTIR) spectroscope (Nicolet iN10 MX infrared imaging microscope, Thermo Scientific, USA) equipped with x-y motorized micro-positioning stage (precision 1 μm) was used to investigate the oxidation behavior of the cross-sections. All the spectra were run in attenuated total reflection (ATR) mode with a 4 cm^{-1} resolution and reported in absorbance (A). The analysis area was allowed to collect on a 10 μm×10 μm surface but 60 μm×60 μm was used in the present study. The line-scan spectra based on 64 scans were carried out with an interval of 200 μm along the radial direction through the microtomed cross-section of the cylinder. Oxidation levels were quantified as an oxidation index (OI), calculated by normalizing the carbonyl absorbance over 1685-1745 cm^{-1} to the reference absorbance over 1330-1390 cm^{-1} wavenumbers according to the ASTM F2102-06$^{\varepsilon 1}$.

The same specimen prepared for the FTIR analysis has also been used for micro-indentation testing. Micro-indents were performed on a DUH-211 dynamic ultra-micro-hardness tester (Shimadzu Corporation, Japan) with a peak load of 100 mN at a loading rate of 13.3 mN/s. After a holding time of 5 s, the load was released at the same constant rate as in the loading cycle. The indentation testing traversed the whole cross-section by a series of 30 indents separated with an interval of 200 μm. The micro-hardness and modulus were calculated according to the ISO 14577-1 (Annex A) by the instrument.

The crystallinity was determined using additional microtomed thin sections (at least n=3 each). Three distinct regions were tested: the surface region, the more oxidized subsurface region, and the less oxidized center region. The samples (around 8 mg each) were sealed in aluminum pans and tested on a Differential Scanning Calorimetry (DSC, X-DSC 7000, SII Nano Technology Co., Ltd., Japan). The sample pan, along with an empty reference pan, was placed in the DSC chamber, which housed two heaters, one for each pan. The heating runs were performed from 30°C to 185°C at a heating rate of 10°C/min under dry nitrogen atmosphere, then cooled

down to 30°C at a cooling rate of 10°C/min. The heat of fusion is calculated by integrating the area under the DSC endothermic peak for the first time. The degree of crystallinity of UHMWPE specimen was calculated by normalizing the heat of melting to that of 100% crystalline PE, by the following equation [20,21]:

$$X_C(\%) = \frac{\Delta H_m}{\Delta H_m^{100}} \times 100 \quad (1)$$

where X_C is the degree of crystallinity, ΔH_m is the heat of fusion corrected for one gram of UHMWPE specimen, ΔH_m^{100} is the heat of fusion for 100% crystalline UHMWPE taken as 290 J/g.

2.3. Multi-directional pin-on-plate wear test

Similar to the DSC tests, three distinct regions were selected to perform the wear tests. The testing samples were machined to a proper shape for the wear tests by using the lathe. The geometry of the test specimen is shown in Fig. 1. The parameters (a, b, c) used for the processing at different regions are based on the results of oxidation behavior of the cross-section measured by FTIR mapping method and shown in Table 1. Before the wear tests, the average OI and micro-hardness of the testing surfaces were measured by FTIR and micro-indentation.

The wear behavior of shelf-aged specimen was evaluated by using a three-station multi-directional sliding pin-on-plate wear tester in which the fixed pin specimen articulates upon the plate specimen surface along a circular path with a diameter of 30 mm [22]. Medical grade cast CoCrMo alloy was used as a plate specimen and polished by using diamond slurry to a surface roughness R_a of 0.01±0.005 μm measured by a stylus roughness meter. Prior to the wear test, both the pin and plate specimens were ultrasonically cleaned in distilled water with a detergent (polyoxyethylene p-t-octylphenylether) for 30 min. Then the specimens were rinsed with a stream of distilled water to remove the detergent and ultrasonically washed again for 30 min with distilled water. Finally, the specimens were washed ultrasonically in ethanol for 15 min and then dried in a vacuum desiccator for 2 h at room temperature.

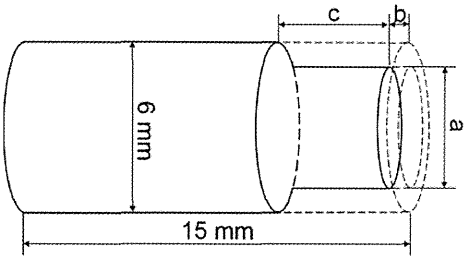

Fig. 1 The geometry of pin specimen

Wear tests were carried out under the lubrication of 30% bovine serum solution at room temperature. A mean contact pressure of 6 MPa and a sliding velocity of 50 mm/s were applied. All experiments were stopped after 10 km sliding distance. The wear amount of the pin specimen was determined from the weight loss. At an interval of 5 km sliding distance, the pin specimen was removed from the test apparatus and cleaned by the same procedure described before. Then the specimen was weighed to an accuracy of 0.01 mg. A static control pin was soaked in the same lubricant to estimate the weight gain due to the fluid uptake from the lubricant. Then, the specific wear rate k ($mm^3N^{-1}m^{-1}$) was calculated by dividing the wear volume ΔV (mm^3) by the sliding distance S (m) and applied normal load F (N) to characterize the wear resistance of the UHMWPE pin specimens. Non-crosslinked UHMWPE without shelf-ageing was used as control.

2.4. Morphology observation

The morphologies of worn surfaces were observed with an optical microscope (Nikon Eclipse LV 150) in bright field and scanning electron microscope (SEM, JEOL JCM-6000). Prior to the SEM observation, the samples were coated with a ~5 nm-thick platinum layer to prevent them from charging. The samples were imaged using secondary electrons at an accelerating voltage of 15 kV.

Table 1 The parameters (a, b, c) of the processing

Material	Regions	Parameter a / (mm)	Parameter b / (mm)	Parameter c / (mm)
Non-crosslinked UHMWPE	surface	6.0	0.0	0.0
Shelf-aged 50 kGy UHMWPE	surface	4.0	0.0	3.0
Shelf-aged 50 kGy UHMWPE	subsurface	3.8	1.1	3.0
Shelf-aged 50 kGy UHMWPE	center	2.8	7.5	3.0
Shelf-aged 100 kGy UHMWPE	surface	4.0	0.0	3.0
Shelf-aged 100 kGy UHMWPE	subsurface	3.8	1.0	3.0
Shelf-aged 100 kGy UHMWPE	center	2.8	7.5	3.0

3. Results

Fig. 2 shows the line-scan ATR spectra collected along the radial direction of the cross-section of the testing samples. Compared with non-irradiated UHMWPE (Fig. 2(a)), the crosslinked UHMWPE spectra (Figs. 2(b), (c)) showed the clear absorptions of acids at 1712 cm^{-1} with shoulder absorptions of esters at 1740 cm^{-1} which can be attributed to C-O stretching. No significant differences were observed between 50 kGy and 100 kGy ATR spectra. The largest absorption intensity of carbonyl groups around 1720 cm^{-1} is at the subsurface for both shelf-aged samples. Along the cross-section, the inhomogeneous presence of acids indicated a depth-dependent oxidation phenomenon of shelf-aged crosslinked UHWMPE.

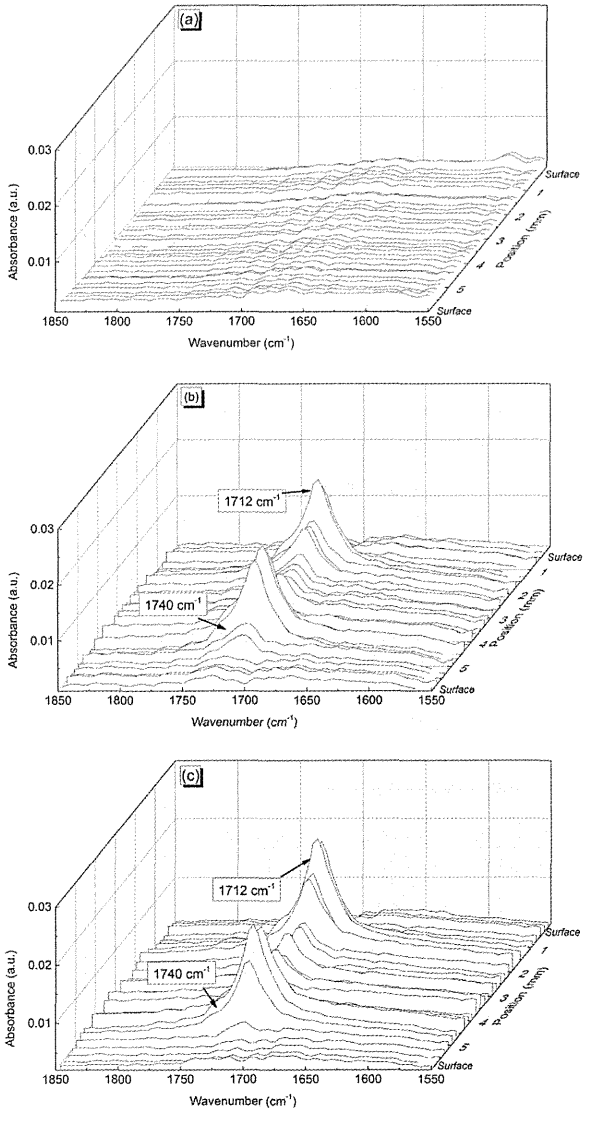

Fig. 2 ATR spectra collected along radial direction of cross-section of non-crosslinked (a), 50 kGy (b) and 100 kGy (c) crosslinked UHMWPE

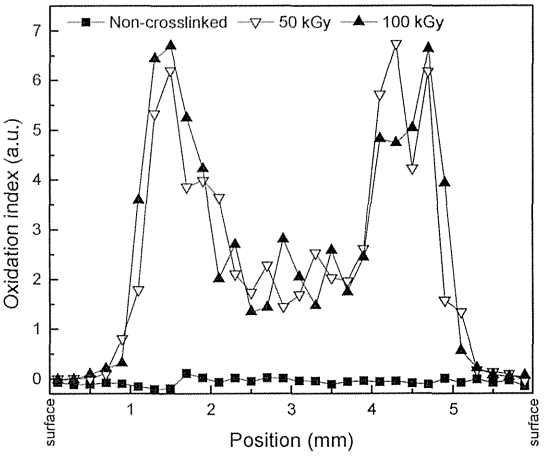

Fig. 3 Oxidation index as a function of position of non-crosslinked and crosslinked UHMWPE

The oxidation index (OI) of testing samples are calculated and plotted against position along the radial direction of the cross-section in Fig. 3. The OI of the non-crosslinked sample showed a relatively low and stable trend through the whole cross-section. Both of the two dose level crosslinked UHMWPE were susceptible to oxidation and showed the similar oxidation index profiles varying with the position after 7-year shelf-ageing. The maximum values of OI for 50 kGy and 100 kGy samples were 6.62 and 6.66, respectively and obtained at around 1.5 mm below the surface. The OI measured close to the surface showed relatively low values in the crosslinked samples, even comparing with the non-crosslinked sample. In addition, as the measurement location near the center, the OI of crosslinked UHMWPEs decreased and showed relatively fluctuant values at center region.

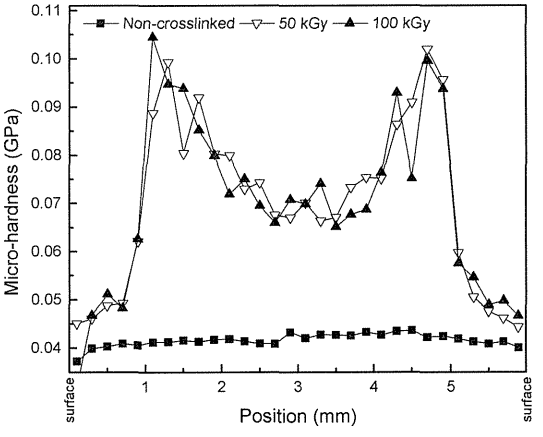

Fig. 4 Micro-hardness as a function of position of non-crosslinked and crosslinked UHMWPE

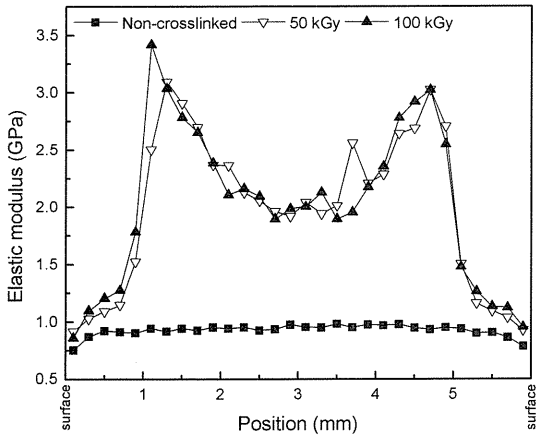

Fig. 5 Elastic modulus as a function of position of non-crosslinked and crosslinked UHMWPE

The micro-indentation test results of non-crosslinked and crosslinked UHMWPE are shown in Fig. 4 and Fig. 5. The profiles of micro-hardness and elastic modulus followed the similar trend as the oxidation index profile and indicated that oxidation behavior had a direct impact on the mechanical properties of shelf-aged crosslinked material. In addition, the two dose levels crosslinked UHMWPEs had the similar maximum value of micro-hardness, which is around 0.10 GPa and elastic modulus, which is around 3.14 GPa. The position of the peaks along the cross-section was at around 1.4 mm below the surface. No significant differences were found between the two shelf-aged crosslinked UHMWPEs.

The average values of OI, micro-hardness and crystallinity for all the testing surfaces measured before the wear tests are shown in Fig. 6 together with the results of the wear tests. Compared with the non-crosslinked sample, the OI, micro-hardness and crystallinity of crosslinked UHMWPE were all higher at the surface regions after 7-year shelf-ageing. The average values of OI, micro-hardness and crystallinity of 50 kGy sample were lower than 100 kGy sample at subsurface and center regions, while different patterns were observed in micro-hardness and crystallinity at surface region.

The specific wear rates at selected regions of non-crosslinked and crosslinked UHMWPE are shown in Fig. 6(d). The results showed that the specific wear rates at high-oxidized regions (subsurface and center region) were two orders of magnitude higher than at the surface regions for crosslinked UHMWPE. Compared with the non-crosslinked sample, the crosslinked samples still maintained excellent wear resistance after 7-year shelf-ageing at the surface region. The specific wear rates of 50 kGy and 100 kGy samples at the surface region were 9.57×10^{-8} and 3.19×10^{-8} $mm^3/(Nm)$ which is about one third and one tenth of the non-crosslinked sample (3.01×10^{-7} $mm^3/(Nm)$), respectively. Moreover, the specific wear rates at subsurface regions and center regions followed the similar trend as the oxidation index,

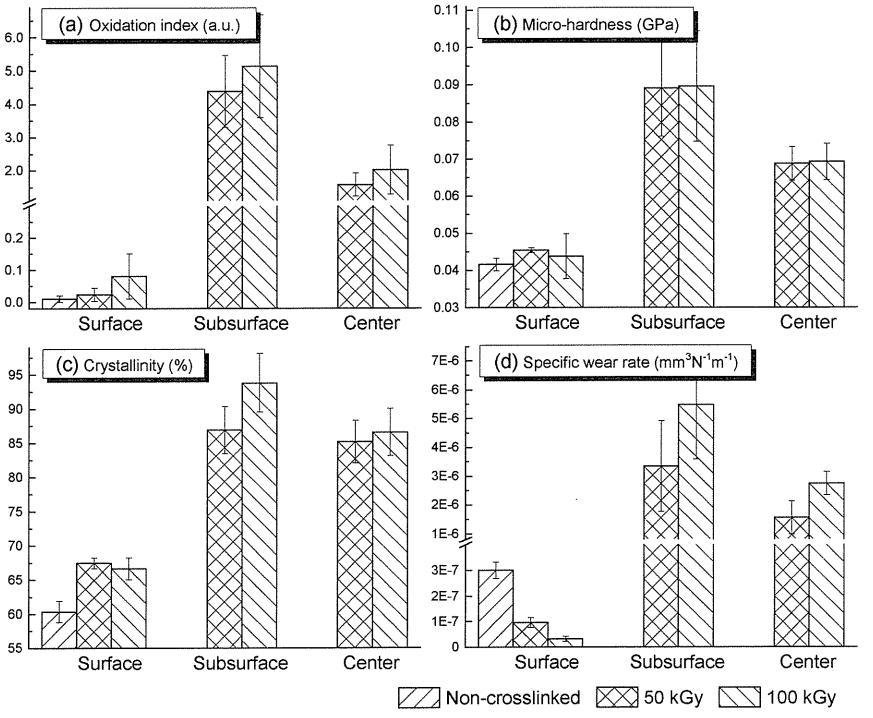

Fig. 6 The OI (a), micro-hardness (b), crystallinity (c) and specific wear rate (d) at the selected testing surfaces of non-crosslinked and crosslinked UHMWPE (mean ± SD, n=3)

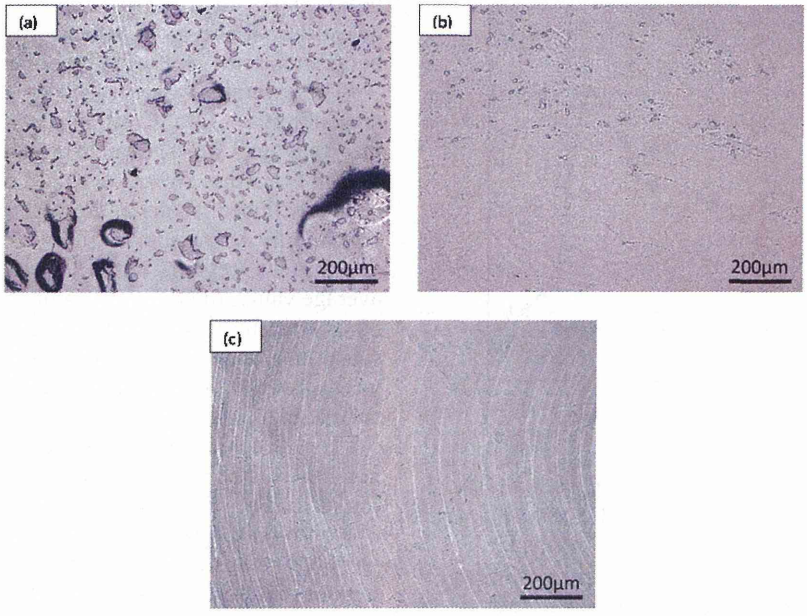

Fig. 7 Appearance of non-crosslinked (a), 50 kGy (b) and 100 kGy (c) worn surfaces at the surface region

micro-hardness and crystallinity.

Fig. 7 shows the morphological characteristics of the UHMWPE worn surfaces at the surface region after the multi-directional sliding tests, observed by optical microscopy. The appearance of the worn surfaces was significantly different between each specimen. No machining marks were observed on the worn morphology of non-crosslinked sample (Fig. 7(a)), but amount of debris and sporadic protuberance were observed. Slight machining marks and a small quantity of debris were the main features of the worn morphology of the 50 kGy sample as shown in Fig. 7(b), while obvious machining marks were observed on the worn surface of the 100 kGy sample (Fig. 7(c)). Morphology observation results were consistent with the results of wear rate.

The fine structure of the worn surface was also examined with the scanning electron microscope (SEM).

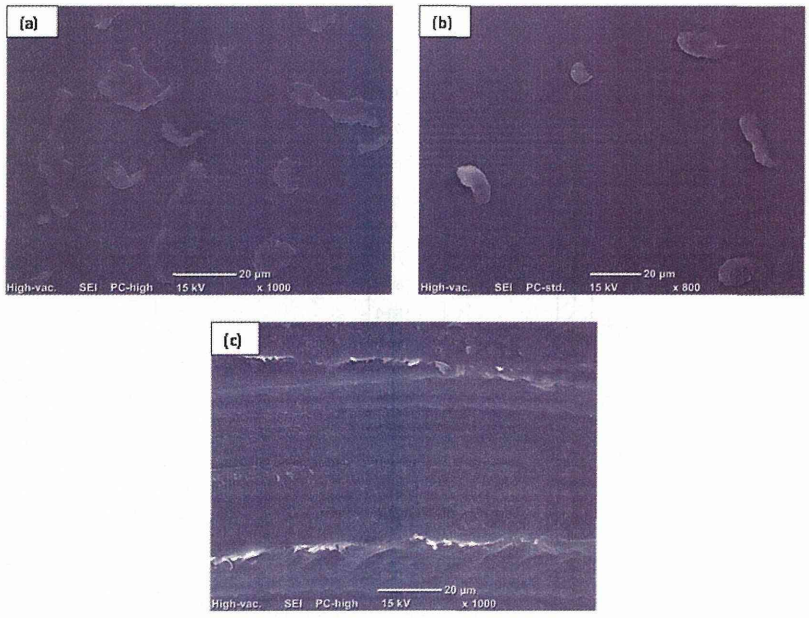

Fig. 8 SEM images of non-crosslinked (a), 50 kGy (b) and 100 kGy (c) worn surfaces at the surface region

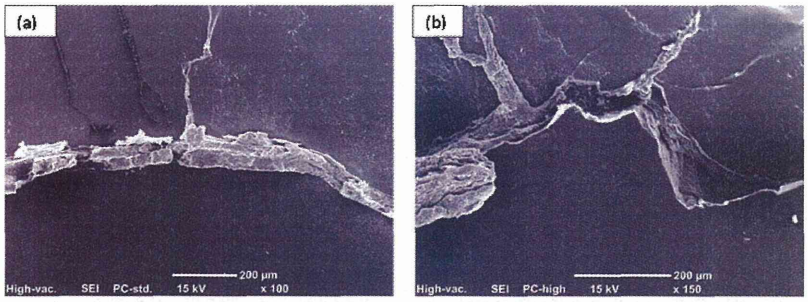

Fig. 9 SEM images of 50 kGy (a) and 100 kGy (b) worn surfaces at the subsurface region

SEM images of worn surfaces at the surface region are shown in Fig. 8. Similar features were observed with the optical microscopy. However, no machining marks were observed on the 50 kGy sample, and the 5 nm-thick platinum coating layer was probably responsible for it. Fig. 9 shows the SEM images of the worn surface at the subsurface region of crosslinked samples. Cracks, fracture and fibril formations were observed on both crosslinked UHMWPE worn surfaces. Compared with the 50 kGy sample (Fig. 9(a)), more cracks and fracture occurred on the 100 kGy sample (Fig. 9(b)), and this may reflect the more serious wear rate of the 100 kGy sample at the subsurface region, which is consistent with the wear rate results (Fig. 6(d)). Furthermore, similar features of masses of fibril formations were observed at the center region of the worn surfaces for both crosslinked samples as shown in Fig. 10.

4. Discussion

Although the link between the oxidation behavior and mechanical properties of crosslinked UHMWPE has been investigated by many studies [18,23], the relationship between the wear rate and oxidation behavior remains unclear.

The results of this study agreed with earlier investigations [13,18,23] that showed the depth-dependent oxidation behavior of crosslinked UHMWPE shelf-aged after gamma-irradiation in air. The results also showed that the profiles of micro-hardness (Fig. 4) and modulus (Fig. 5) along the cross-section of crosslinked samples mirrored the OI profile (Fig. 3). It indicated that the effect of oxidation on the mechanical properties of shelf-aged crosslinked UHMWPE was strong and direct. The maximum value of OI, micro-hardness and elastic modulus of gamma-irradiated UHMWPE occurred at the subsurface (Figs. 2-5). The highly oxidized subsurface region was recognized as a circular band with a distinctive white color in the microtomed slices as shown in Fig. 11 and usually called "white band" [24]. The embrittled subsurface white band is susceptible to cracking and delamination, which would be the critical element to cause early failures of the artificial joint.

The correlation between the wear rate and oxidation index was shown in Fig. 12. The figure indicated that the wear rate of the crosslinked UHMWPE was significantly increased with increasing OI. Worn surface morphology observation showed that the surface regions of shelf-aged samples (Fig. 7) still have some machining marks. However, the subsurface regions of shelf-aged samples (Fig. 9) showed fracture, cracks and more severe wear patterns and the machining marks totally disappeared. The center regions showed moderate wear patterns; the removal of machining marks and formation of many

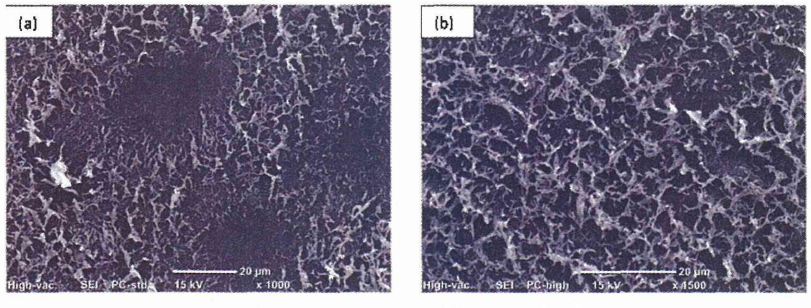

Fig. 10 SEM images of 50 kGy (a) and 100 kGy (b) worn surfaces at the center region

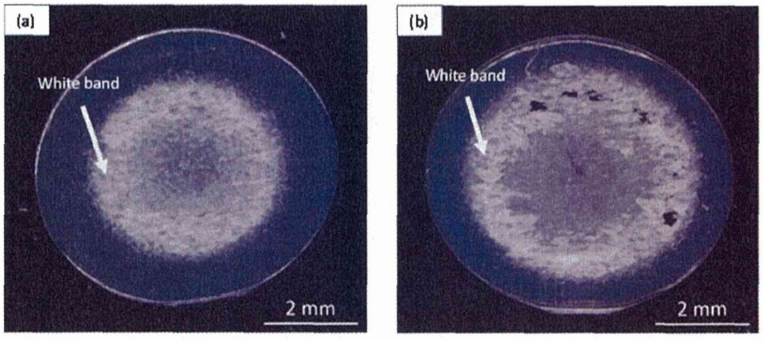

Fig. 11 Optical micrographs of microtomed 50 kGy (a) and 100 kGy (b) UHMWPE slices

fibrils without cracks and fractures. Therefore, the characteristics in the worn surface morphology of each region coincided with the evaluated specific wear rate and both values certainly related to the OI.

How could the higher oxidation result in the degradation of wear resistance in the gamma-irradiated UHMWPE. Gamma radiation is supposed to form the UHMWPE crosslinks to improve the wear-resistance of this polymer [6]. However, gamma irradiation of polyethylene components, which dissociates molecular bonds, not only leads to crosslinking but also induces the formation of residual free radicals [9,12]. The reaction between residual free radicals and diffused oxygen molecules initiates a significant concentration of peroxy radicals to start the oxidative degradation in UHMWPE. With ageing, oxygen diffuses deep into the UHMWPE components, reacts with the free radicals and eventually causes more oxidation. This process results in a higher oxidation index and lower molecular weight at the subsurface. The shortened molecular chains enhance the chain mobility and provide more chance of recrystallization by crystal perfection processes, thus the degree of crystallinity of UHMWPE increases following oxidation (Fig. 6(c)). Consequently, the mechanical properties, such as micro-hardness and elastic modulus, increased since they are depended on the crystallinity in many kinds of polymers (Fig. 6(b)). Meanwhile, the shortened molecular chains also reduce the abrasion resistance of polymer materials due to the reduction of the molecular weight, which is an important factor increasing the strength and wear resistance of polymers. In addition, recrystallization process, which was caused by the oxidation, results in polymer shrinkage in the same volume [24]. This phenomenon will cause a rough, brittle and porous microstructure (Fig. 11) in the material. Such a deteriorated microstructure is supposed to be the main reason for the highest wear rate at the most oxidized subsurface region.

Interestingly, Fig. 12 showed that the slope of the graph increased as the radiation dose increased. Researchers [11,13] pointed out that the radiation dose has a certain effect on the oxidation and mechanical properties of crosslinked UHMWPE, due to the difference in the crosslink density induced by the different dose level of gamma irradiation. Thus, the crosslink density may play a certain role in the dose dependent wear behavior of gamma-irradiated UHMWPE confirmed in our multidirectional wear tests.

In our present work, at surface region with the lowest OI values, the specific wear rate of UHMWPE decreased with increasing the radiation dose. In general with increasing radiation dose, there is an increase in crosslink density. The 100 kGy sample with higher crosslinked density could therefore enjoy a lower wear rate at the surface region. The morphologies at the surface region are also suggesting significant effects of the radiation dose on the wear mechanism of UHMWPE. Amount of debris and sporadic protuberances were all imaged at the worn surface of non-crosslinked sample (Fig. 7(a) and Fig. 8(a)). Less or lightly these features were observed on the 50 kGy worn surface (Fig. 7(b) and Fig. 8(b)). All these features are related to the adhesive wear

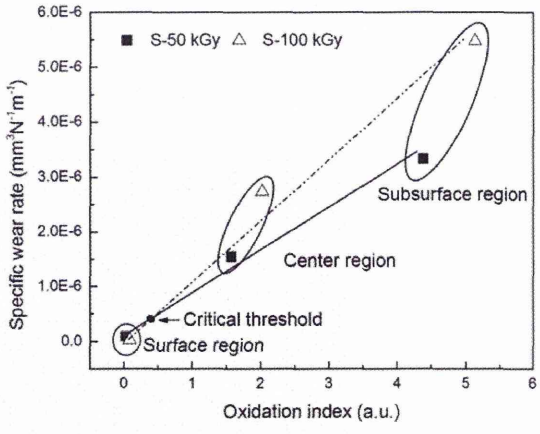

Fig. 12 The relationship between the specific wear rate and oxidation index of crosslinked UHMWPE